Molecular Dynamics of iso-Butyl Alcohol Inside Zeolite H-ZSM-5 as Studied by Deuterium Solid-State NMR Spectroscopy

ARTICLE *in* THE JOURNAL OF PHYSICAL CHEMISTRY B · JULY 2000

Impact Factor: 3.3 · DOI: 10.1021/jp000581e

3 AUTHORS, INCLUDING:

Alexander G Stepanov
Boreskov Institute of Catalysis
135 PUBLICATIONS **1,658** CITATIONS
SEE PROFILE

Aleksandr A. Shubin
Boreskov Institute of Catalysis
85 PUBLICATIONS **1,232** CITATIONS
SEE PROFILE

Molecular Dynamics of *iso*-Butyl Alcohol Inside Zeolite H-ZSM-5 as Studied by Deuterium Solid-State NMR Spectroscopy

Alexander G. Stepanov,*,† Maxim M. Alkaev,‡ and Alexander A. Shubin†

Boreskov Institute of Catalysis, Siberian Branch of the Russian Academy of Sciences, Prospekt Akademika Lavrentieva 5, Novosibirsk 630090, Russia, and Department of Physics, Novosibirsk State University, Pirogova Street 2, Novosibirsk 630090, Russia

Received: February 14, 2000; In Final Form: May 18, 2000

The molecular mobility of *iso*-butyl alcohol, selectively deuterated in the methylene group (iBA[1-d_2]) or in the methyl groups (iBA[3-d_6]), adsorbed on zeolite H-ZSM-5 was studied with ^{2}H NMR spectroscopy. At 115−293 K, the ^{2}H NMR line shape for the adsorbed iBA[3-d_6] represents a superposition of one solidlike and two liquidlike signals, whereas for iBA[1-d_2], it is a superposition of the solidlike and the liquidlike lines. Two liquidlike signals are assigned to the alcohol molecules isotropically reorienting with correlation time $\tau_R \sim 1 \times 10^{-6}$ s by jumping among Al−OH−Si groups, which are located inside the channels and at channel intersections of the zeolite channel system. Being adsorbed on Al−OH−Si groups, these two types of alcohol molecules differ in the effective amplitude of libration γ_0 (γ_0 is a libration cone semiangle) of the methyl groups, which is large for both adsorption sites ($\gamma_0 \sim 52°$ for one of the types, and $\gamma_0 \sim 72°$ for the other). The solidlike signal with the observed quadrupole splitting of 38 kHz is assigned to the alcohol molecules located inside the zeolite channels. These alcohol molecules reorient with a correlation time $\tau_R > 4.2 \times 10^{-6}$ s, and their methyl groups experience small librations with amplitude $\gamma_0 \sim 19°$. Methyl groups of the alcohol molecules located at channel intersections rotate about the CH_3−CH axis with correlation time $\tau_P = (1.4-2.6) \times 10^{-11}$ s at 293 K and activation energy $E_P = 11-12$ kJ/mol, whereas those located inside the channel rotate with correlation time $\tau_j \sim 2 \times 10^{-10}$ s at 293 K and activation energy $E_j = 10.5$ kJ/mol. The difference in the rotation rates is attributed to the influence of the walls of the zeolite channel on dynamics of one-axis methyl group rotation, which is expected to be more profound in the confined area of a narrow channel than at channel intersections.

Introduction

Deuterium solid-state NMR (^{2}H NMR) has been demonstrated many times to be a powerful tool for monitoring the mobility of organic molecules occluded in zeolite pores.[1−13] The dynamics of aromatic molecules,[1,2,4,7,8] alcohols,[2,3,11] olefins,[5,6,10] and alkanes[9,12,13] have been probed with the aim of clarifying the peculiarities of the dynamic behavior of these species in the constrained area of the zeolite pores. The mobility of alkanes and aromatic molecules (benzene, xylenes), which weakly interact with the walls of zeolite pores or channels and whose dimensions are commensurate to the sizes of zeolitic pores, is strongly influenced by the regular periodicity of the zeolitic pore system.[7,8] At the same time, the mobility of alcohols is influenced by the alcohol interaction with the Brönsted acid sites of the zeolites.[3] Therefore, the local motion of the alcohol physically adsorbed on the acid sites may strongly contribute to the motional behavior of the adsorbed alcohols. Qualitative interpretations of the ^{2}H NMR data were offered for the previously studied alcohols,[2,3,11] mainly in terms of the superposition of two components contributing to the total ^{2}H NMR line shape, corresponding to mobile and immobilized alcohol molecules.

Meanwhile, quantitative information on the mobility of alcohol molecules, whose dimensions are commensurate with the sizes of the zeolite pores and whose dynamics are strongly affected by the zeolitic walls, the regular periodicity of the zeolitic pore system, and interactions with zeolite acid sites, may lead to elucidation of the origin of the shape selectivity of zeolites[14] in catalytic reactions and may provide the basis for the development of models for alcohol molecule diffusion and for clarification of the mechanism of this diffusion.

Studies of butyl alcohols adsorbed on zeolite ZSM-5 have received particular attention for the past several years.[11,15−18] The reasons are mainly the following. First, dehydration of these alcohols is a good model reaction for mechanistic studies of alcohol conversion on zeolites, including identification of the intermediates (carbenium ions and/or alkoxide species) and clarification of their role in this reaction.[15,16a,16d,18] Second, because the dimensions of butyl alcohols are commensurate with the diameters of the channels of zeolite ZSM-5 (5.5 Å),[19] C_4 alcohols are ideally suited for a study of pore confinements,[16b,16c,18] which are the basis for the shape selectivity of zeolites.[14]

In this paper, the mobility and localization of *iso*-butyl alcohol inside the channel system of zeolite H-ZSM-5 was studied using ^{2}H NMR spectroscopy[20−22] with the aim of clarifying the influence of both the zeolite walls (pore confinement effect) and the interaction with zeolite acid sites on the motional behavior of the adsorbed alcohol molecules. To monitor selectively the dynamics of either the alcohol molecule as a whole or only the separate methyl groups, *iso*-butyl alcohol, selectively deuterated either in methylene group (iBA[1-d_2]) or in the methyl groups (iBA[3-d_6]) was used in this study.

* Corresponding author. Fax: +7 3832 34 30 56. E-mail: a.g.stepanov@catalysis.nsk.su.

† Siberian Branch of the Russian Academy of Sciences.

‡ Novosibirsk State University.

10.1021/jp000581e CCC: $19.00
Published on Web 07/25/2000

Experimental Section

Materials. Two samples of zeolite H-ZSM-5 with Si/Al = 29 and Si/Al = 24 were prepared from Na-ZSM-5 via NH_4^+ ion exchange and subsequent calcination at 550 °C, as described in ref 23. The crystallinity of the samples was verified by X-ray powder diffraction. Both samples were found to be highly crystalline, i.e., to contain no amorphous phase. Scanning electron microscopy micrographs of both ZSM-5 zeolite samples showed that these samples represented roughly prismatic crystals, which made up secondary spherical aggregates, with diameters ranging from 7 to 8 μm. According to chemical analysis, the content of Fe^{3+} admixtures was 23 ppm in both samples. The overall amount of Al in the sample was assumed to be equal to that found from chemical analysis. The ratio between the integral intensities of ^{27}Al MAS NMR signals at +54 ppm [tetrahedral Al, $Al(H_2O)_6^{3+}$ as the chemical shift reference] and at −2.5 ppm (octahedral Al)[24] corresponds to contents of 6% and 7% octahedral Al and 94% and 93% tetrahedral Al relative to the overall amount of Al (tetrahedral + octahedral) in the zeolite for the samples with Si/Al = 29 and Si/Al = 24, respectively. For the sake of simplicity, ^{27}Al MAS NMR spectra were recorded with the samples that were kept in air atmosphere for a long time and were not subjected to any special treatment before the ^{27}Al NMR measurements. The absolute concentration of tetrahedral Al in the samples with Si/Al = 29 and Si/Al = 24 was, respectively, 458 and 527 μmol per 1 g of the zeolite, which was kept in air. As was shown by the special experiment, these undehydrated zeolite samples contained 7.7 wt % of atmospheric moisture.

Both *iso*-butyl alcohol, selectively deuterated in the methylene group $\{(CH_3)_2CHCD_2OH$, iBA[1-d_2], 96% ^{2}H enrichment] and *iso*-butyl alcohol, selectively deuterated in the methyl groups $\{(CD_3)_2CHCH_2OH$, iBA[3-d_6], 99.6% ^{2}H enrichment} contained less than 1.5% residue of diethyl ether, coming to the alcohols during the procedures of their synthesis.

Samples Preparation. To prepare the samples for NMR experiments, approximately 0.7 g of zeolite was loaded in a 10-mm (o.d.) glass tube, which was connected to a vacuum system by a narrow neck. The sample was then heated at 450 °C for 1.5 h in air and for 4 h under vacuum to a final pressure above the sample of 10^{-5} Torr (1 Torr = 133.3 Pa). After the sample was cooled back to room temperature (22 °C), zeolite was exposed to the vapor of previously degassed alcohol (ca. 4 Torr, according to a mercury manometer) in the calibrated volume (138.5 mL). It took a few minutes for complete consumption of *iso*-butyl alcohol vapor to occur. The procedure of adsorption was repeated several times until the desired amount of adsorbed alcohol was achieved, i.e., 200−300 μmol/g (2−2.5 wt %). The adsorbed quantity of the alcohol was approximately two times less than the amount of tetrahedral Al. After the adsorption was over, the sample was immediately placed into liquid nitrogen to prevent a possible reaction of alcohol dehydration at room temperature.[16a] Following this step, the neck of the tube was sealed off, while zeolite sample was still maintained in liquid nitrogen in order to prevent its heating by flame. After that, the sealed sample was kept in liquid nitrogen and then transferred into a precooled NMR probe just before recording of the ^{2}H NMR spectra.

NMR Measurements. ^{2}H NMR experiments were performed at 61.42 MHz on a Bruker MSL-400 spectrometer, using a high-power probe with a 10-mm horizontal solenoid coil. All ^{2}H NMR spectra were obtained by Fourier transformation of the quadrature-detected quadrupole echo, arising in the pulse sequence[25]

$$(\theta_1)_{\pm X}-\tau_1-(\theta_1)_Y-\tau_2-\text{acquisition}-t \qquad (i)$$

where $\tau_1 = 30$ μs, $\tau_2 = 36$ μs, and t is the repetition time for the sequence i during the accumulation of NMR signal. Radio frequency pulses of 4.0−4.5 μs in length, which corresponds to $\theta_1 = 70-75°$, were used. Under conditions of our experiments, some loss of the signal intensities and distortion of the shape of the observed NMR lines took place because of finite pulse lengths and time delays.[26,27] However, the expected distortions did not affect the basic results and conclusions of the present study.

Spectra were typically obtained with 500−5000 scans and a repetition time of 0.4−2 s. Inversion−recovery experiments for spin−lattice relaxation time T_1 measurements were carried out by using the sequence

$$(\pi)_X-t_V-\left(\frac{\pi}{2}\right)_{\pm X}-\tau_1-\left(\frac{\pi}{2}\right)_Y-\tau_2-\text{acquisition}-t \qquad (ii)$$

where the length of the $\pi/2$ pulse is 5.0−5.4 μs and t_V is a variable delay between the 180° $(\pi)_X$ inverting pulse (as in the standard inversion−recovery pulse sequence[28]) and the quadrupole-echo sequence i. In the case of the overlapping of different signals with liquidlike line shapes that contribute to the overall ^{2}H NMR spectrum, T_1 values were estimated on the basis of the time τ_0 ($\tau_0 = T_1 \ln 2$). τ_0 is the time at which the intensity of the NMR line turns from the inverted negative position to the normal positive position in the inversion−recovery experiment *ii*.

The temperature of the samples was controlled with a flow of nitrogen gas, and stabilized with a variable-temperature unit BVT-1000 with a precision of about 1 K.

Theoretical Background. ^{2}H NMR spectra of polycrystalline organic solids are known to be dominated by quadrupole coupling.[20−22,29−32] This coupling is mainly of intramolecular origin[20−22] and is strongly affected by the mode and the rate of the molecular motion in which a molecule is involved.[20,29−33]

For molecules that are rigid on the ^{2}H NMR time scale,[33] $\tau_{NMR} \sim [(3/4)2\pi Q_0]^{-1}$, where $Q_0 = e^2qQ/h$ is the quadrupole coupling constant), the ^{2}H NMR spectra represent Pake-type powder patterns.[20,21] The dominant features of these line shapes are two sharp peaks separated by the distance $(3/4)Q_0$ and two shoulders separated by $(3/2)Q_0$ (Figure 1A). For deuterium bonded to tetrahedral carbon atoms in polycrystalline organic solids, $(3/4)Q_0$ is usually 120−130 kHz, while the principal axis of the quadrupole coupling tensor has a direction close to that of the C−D bond, and the asymmetry parameter η is close to zero.[29−34] If a CD_3 group of an organic molecule undergoes fast rotational diffusion or random jumps about the 3-fold axis (e.g., about C−CD_3 bond) with the characteristic correlation time $\tau_C \ll [(3/4)2\pi Q_0]^{-1}$, and if additional isotropic reorientation of the molecule as a whole, τ_R, is slow, i.e., $\tau_R \gg [(3/4)2\pi Q_0]^{-1}$, then the line shape of the ^{2}H NMR spectrum of the CD_3 group will be similar to that for a rigid molecule, but with the quadrupole splitting reduced (see Figure 1B) according to equation

$$\frac{3}{4}Q_1 = \frac{3}{4}Q_0\left(\frac{3\cos^2\rho - 1}{2}\right) \qquad (1)$$

Here, ρ is the angle between the C−D bond and the axis of rotation (C−CD_3 bond). For the ideal tetrahedral geometry of the C−CD_3 fragment, $\rho = \arccos(1/3) = 70.53°$, and $Q_1 = (1/$

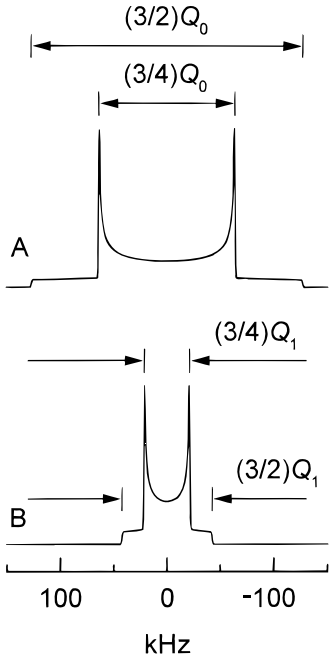

Figure 1. Theoretical ^{2}H NMR spectra. (A) Polycrystalline sample (static CD_3 group, $Q_0 = e^2qQ/h = 170$ kHz, $\eta = 0$, $T_2^{-1} = 630$ s^{-1}). (B) Rapid rotation of the CD_3 group about one C_3 axis, angle $\rho = 70.53°$, $T_2^{-1} = 630$ s^{-1}.

$3)Q_0$. In practice, typical values of the reduced splitting are $(^3/_4)Q_1 = 35-40$ kHz.[30−35] If a rapidly rotating CD_3 group of a fixed or slowly tumbling molecule undergoes additional local motion, such as fast librations of the C−CD_3 bond, then the observed value of $(^3/_4)Q_1$ will be defined as follows

$$\frac{3}{4}Q_1 = \frac{3}{4}Q_0 S\left(\frac{3\cos^2\rho - 1}{2}\right) \tag{2}$$

In this equation, a fast librational motion is taken into account by the order parameter S, which depends on the deviation of the rotation axis from its mean position

$$S = \left\langle \frac{3\cos^2\gamma - 1}{2} \right\rangle \tag{3}$$

where γ is the angle between the instantaneous and the mean orientation of the rotation C−CD_3 axis during libration and pointed brackets denote the average over the librational motion.

Evaluation of the order parameter S requires a detailed knowledge of the librational angle distribution function,[24] which usually is not available. To get an estimation of the magnitude of the libration angles, the model of "free diffusion in a cone" can be applied. Within the framework of this model, the order parameter S_{cone} can be expressed as[36,37]

$$S_{cone} = \frac{\cos\gamma_0\,(1 + \cos\gamma_0)}{2} \tag{4}$$

where γ_0 $(0 \le \gamma \le \gamma_0)$ is the cone semiangle, which can be obtained from eq 4 in the following way

$$\gamma_0 = \arccos\left[\frac{(1 + 8S_{cone})^{1/2} - 1}{2}\right] \tag{5}$$

When the correlation time τ_R for the isotropic reorientation of the molecule as a whole becomes comparable to the inverse value of Q_0, i.e., $\tau_R \approx [(^3/_4)2\pi Q_0]^{-1}$, a broadening of the spectrum is observed, and the sharp features are washed out.[21] For rapid isotropic reorientation, as in liquids, i.e., when $\tau_R \ll [(^3/_4)2\pi Q_0]^{-1}$, quadrupole splitting is averaged to zero, and a single line of Lorentzian shape is observed at ν_0. For $\eta = 0$, the width of this line is given by the formula[22]

$$\Delta\nu_{1/2} = \frac{1}{\pi T_2} = \frac{3\pi}{100}\frac{2I+3}{I^2(2I-1)}Q_0^2[3\tau_R + 5g(\tau_R,\omega_I) + 2g(\tau_R,2\omega_I)] \tag{6}$$

where $I = 1$, $g(\tau,\omega) = \tau/[1 + (\omega\tau)^2]$, $\tau_R = 1/(6D_{rot})$, D_{rot} is the rotational diffusion coefficient for isotropic reorientation, $\omega_I = 2\pi\nu_0$, and ν_0 is the Larmor frequency of the deuterium nucleus.

Although the ^{2}H NMR line shape provides information about the type of motion of the CD_3 group in a molecule, it contains no further information about the rate of this process when this anisotropic motion is fast on the ^{2}H NMR time scale. Additional information can be obtained from an analysis of the ^{2}H NMR spin−lattice relaxation time T_1. For fixed molecules with internal motions, Torchia and Szabo[38] have developed explicit expressions for the ^{2}H NMR T_1 values for two different types of methyl group motion, free rotational diffusion about the C−CD_3 axis and random rotational jumps between neighboring positions.

If the CD_3 group diffuses freely with diffusion coefficient $D_{||}$ about the C−CD_3 bond in the absence of overall molecule motion, i.e., $\tau_R \gg [(^3/_4)2\pi Q_0]^{-1}$, then T_1 can be represented as follows[38]

$$\frac{1}{T_1} = \frac{3\pi^2}{10}\frac{2I+3}{I^2(2I-1)}Q_0^2\{\sum_{\substack{m=-2\\(m\neq 0)}}^{2}[d^{(2)}_{1m}(\chi)]^2\,[d^{(2)}_{m0}(\rho)]^2\,g(\tau_m,\omega_I) + 4\sum_{\substack{m=-2\\(m\neq 0)}}^{2}[d^{(2)}_{2m}(\chi)]^2\,[d^{(2)}_{m0}(\rho)]^2\,g(\tau_m,2\omega_I)\} \tag{7}$$

where $\tau_m = 1/(D_{||}m^2)$, $d^{(2)}_{m0}(\theta)$ is the Wigner rotation matrix element, χ is the angle between the C−CD_3 axis and the magnetic field $\mathbf{B}_0$, and ρ ($\cos\rho \sim {}^1/_3$) is an angle complementary to the close-to-tetrahedral C−C−D valence angle. Note, that formula 7 is given here in a different, but completely equivalent, form to that originally presented in ref 38.

If the CD_3 group randomly jumps about the C−CD_3 bond between three equivalent sites rather than moving by rotational diffusion, then the results for the spin−lattice relaxation time can be also represented in a similar form[38]

$$\frac{1}{T_1} = \frac{3\pi^2}{10}\frac{2I+3}{I^2(2I-1)}Q_0^2\{g(\tau_j,\omega_I)\sum_{\substack{m=-2\\(m\neq 0)}}^{2}[d^{(2)}_{1m}(\chi)]^2\,[d^{(2)}_{m0}(\rho)]^2 + 4g(\tau_j,2\omega_I)\sum_{\substack{m=-2\\(m\neq 0)}}^{2}[d^{(2)}_{2m}(\chi)]^2\,[d^{(2)}_{m0}(\rho)]^2 - 2\cos[3(\xi+\varphi_0)]\sin^3\chi\cos\chi\,d^{(2)}_{10}(\rho)\,d^{(2)}_{20}(\rho)\,[g(\tau_j,\omega_I) - g(\tau_j,2\omega_I)]\} \tag{8}$$

where $\tau_j = 1/(3k)$ and k is the rate constant for jumps between neighboring sites. The orientation of the molecule in the laboratory system is described by the angles (ψ, χ, ξ) (first, rotation by the angle ψ about the Z axis; second, rotation by the angle χ about the Y′ axis; and third, rotation by the angle ξ about the Z'' axis). The angle φ_0 defines the jump site positions ($\varphi_n = \varphi_0 + 2\pi n/3$ where $n = 0$, 1, and 2). It is assumed in eq

8 that, for the particular case of $\psi = \chi = \xi = 0$, when the direction of the C−CD_3 bond coincides with the laboratory Z axis, one of the three C−D bonds in CD_3 group has the direction

$$\begin{pmatrix} \sin\rho\cos\varphi_0 \\ \sin\rho\sin\varphi_0 \\ \cos\rho \end{pmatrix}$$

Let us assume that the molecule with the CD_3 group rapidly and freely diffusing about the C−CD_3 axis (with the rotational diffusion coefficient $D_{||}$) also undergoes fast librations ($D_\perp$), and at the same time, the overall reorientation rate of the molecule is also fast on the ^{2}H NMR time scale (i.e., the condition $D_\perp$, $D_{||} \gg D_{rot} > (^3/_4)2\pi Q_0$ is fulfilled). Approximating librations of the the C−CD_3 axis by the free diffusion in a cone model and assuming exactly tetrahedral C−CD_3 geometry, we have derived, in a way similar to described in ref 39, the following expression for the relaxation time T_1

$$\frac{1}{T_1} = \frac{4\pi^2}{1800}\frac{2I+3}{I^2(2I-1)}Q_0^2\{S^2[3(g(\tau_{10},\omega_I) + 4g(\tau_{10},2\omega_I)) + 8(g(\tau_{11},\omega_I) + 4g(\tau_{11},2\omega_I)) + 16(g(\tau_{12},\omega_I) + 4g(\tau_{12},2\omega_I))] + (1-S^2)[3(g(\tau_{20},\omega_I) + 4g(\tau_{20},2\omega_I)) + 8(g(\tau_{21},\omega_I) + 4g(\tau_{21},2\omega_I)) + 16(g(\tau_{22},\omega_I) + 4g(\tau_{22},2\omega_I))]\} \quad (9)$$

where $1/\tau_{1m} = 1/\tau_R + m^2/(6\tau_P)$, $1/\tau_{2m} = 1/\tau_{1m} + (6 - m^2)/(6\tau_S)$ for $m = 0$, 1, and 2. Here, τ_P is an *effective* correlation time for free diffusion of the CD_3 group about −C−CD_3 axis, τ_S is an *effective* correlation time for −C−CD_3 axis movement (libration) in the azimuthally symmetric potential, and S is the order parameter. Under some assumptions,[40] it is possible to translate *effective* correlation times τ_P and τ_S into diffusion constants $D_{||}$ and $D_\perp$ by the formal relations

$$D_{||} = \frac{1}{6\tau_P} \text{ and } D_\perp = \frac{1-S^2}{6\tau_S} \quad (10)$$

Below we will often use the characteristic correlation time $\tau_{||}$ for the rotation of the CD_3 group about C−C axis. Note that $\tau_{||} \sim D_{||}^{-1}$ in the case of rotational diffusion (formulas 7, 9, and 10), and $\tau_{||} \sim \tau_j = 1/(3k)$ for the three-site jump model (formula 8).

A schematic representation of the possible motions for both the methyl groups and the molecule as a whole, which can be monitored by ^{2}H NMR in *iso*-butyl alcohol adsorbed on H-ZSM-5, is provided in Figure 2.

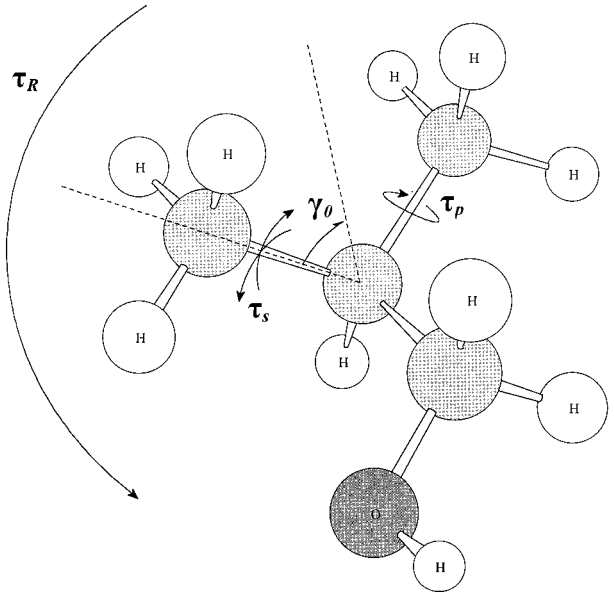

Figure 2. Possible motions for methyl groups and the molecule as whole that can be monitored by ^{2}H NMR spectroscopy in *iso*-butyl alcohol adsorbed on H-ZSM-5.

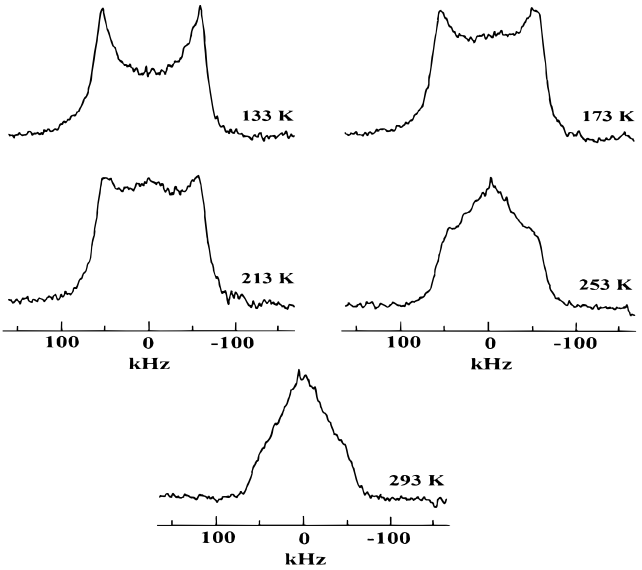

Figure 3. Temperature dependence of ^{2}H NMR line shape for the CD_2 group of iBA[1-d_2] adsorbed on H-ZSM-5 (Si/Al = 29). The amount of adsorbed alcohol is 222 μmol/g.

Results

^{2}H NMR Spectra of the Adsorbed iBA[1-d_2]. Figure 3 shows the variation with temperature of the ^{2}H NMR spectrum of *iso*-butyl alcohol, selectively deuterated in the methylene group, iBA[1-d_2], adsorbed on H-ZSM-5. It is seen that, at 133 K, the CD_2 group of iBA[1-d_2] exhibits a solidlike NMR line shape with a quadrupole splitting of $(^3/_4)Q_0 = 114$ kHz. Both the observed line shape and the quadrupole splitting are slightly different from those typical for rigid molecules (120−130 kHz; see, e.g., Figure 1A and refs 31−34). It is reasonable to assume that the line shape reflects the molecular motion in which the CD_2 group of the alcohol is involved. The distortion of the observed line shape from that typical for a rigid molecule may arise from libration of the C−O bond in the −CD_2OH fragment of the molecule or/and from sluggish, close-to-isotropic reorientation of the molecule as a whole. If we assume that the distortion of the solidlike line shape is due to the contribution to the signal from isotropic-like reorientation, we, nevertheless, should assume that the correlation time for isotropic reorientation of the adsorbed alcohol molecule exceeds the inverse value of the quadrupole splitting, $\tau_R > [(^3/_4)2\pi Q_0]^{-1}$, i.e., $\tau_R > 1.3 \times 10^{-6}$ s. Otherwise, liquidlike lines shape should be observed. At 173 K, a new signal (in addition to the solidlike one) contributing to the observed NMR spectrum appears. This new signal exhibits a liquidlike line shape. It corresponds to either close-to-isotropic or entirely isotropic reorientation of the adsorbed alcohol molecules, i.e., $\tau_R < [(^3/_4)2\pi Q_0]^{-1}$. The integral intensity of the liquidlike signal increases with temperature, whereas that of the solidlike signal decreases (Figure 3). The line width of the liquidlike signal changes only slightly within the temperature range 253−293 K, and it is 45 kHz at 293 K. Using eq 6 for the line width of the isotropically reorienting molecule and taking into account the typical value of $Q_0 = 165$

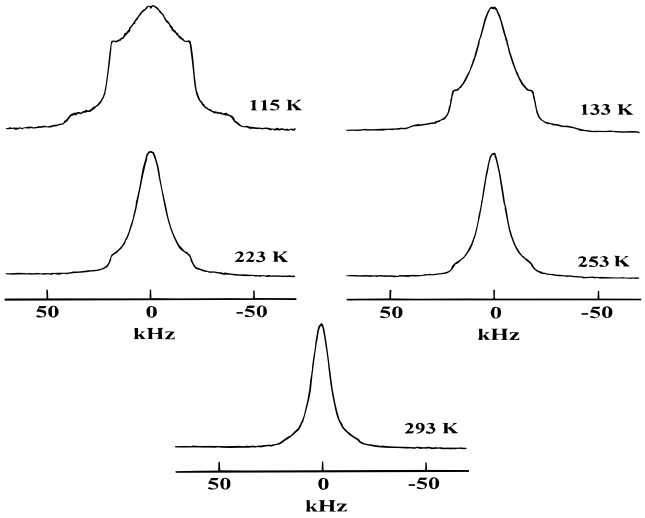

Figure 4. Temperature dependence of ^{2}H NMR line shape for the CD_3 group of iBA[3-d_6] adsorbed on H-ZSM-5 (Si/Al = 24). The amount of adsorbed alcohol is 500 μmol/g.

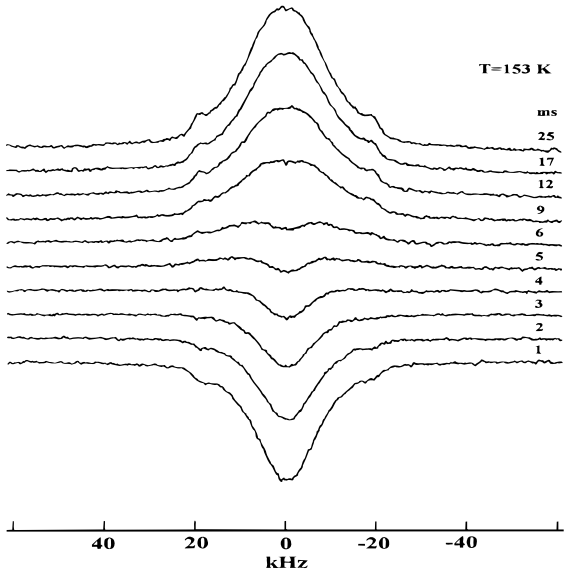

Figure 5. ^{2}H NMR inversion−recovery spectra recorded at 153 K for the CD_3 group of iBA[3-d_6] adsorbed on H-ZSM-5 (Si/Al = 24). The amount of adsorbed alcohol is 287 μmol/g. The delay time t_V (ms) is given above each spectrum.

kHz[31,32] and the observed change of the line width within the temperature range 253−293 K, we can roughly estimate the correlation time for the isotropic reorientation of the alcohol, reflected in the liquidlike line shape, as is $\tau_R \leq 1.2 \times 10^{-6}$ s at 293 K. We can also estimate the upper limit for the activation energy for this mode of motion, which is ∼3 kJ/mol in this case (it is difficult to perform complete line shape analysis because signals overlap and we have to use eq 6 for estimations). Thus, it is possible to clearly distinguish two line shapes for iBA[1-d_2] in H-ZSM-5 within the temperature range 133−293 K. These line shapes reflects different dynamic behavior of the methylene group of the adsorbed alcohol. The solidlike line shape corresponds to the alcohol as a whole, which is almost rigid on ^{2}H NMR time scale. It reorients isotropically with $\tau_R \geq 1.3 \times 10^{-6}$ s. The liquidlike line shape corresponds to the alcohol reorienting a bit faster with $\tau_R \sim 10^{-6}$ s at 253−293 K. It is reasonable to assume that these two line shapes are related to two adsorption states of the alcohol inside the framework of the zeolite.

^{2}H NMR Spectra of the Adsorbed iBA[3-d_6]. Similar variations of the ^{2}H NMR spectrum are observed for the alcohol selectively deuterated in the methyl groups, iBA[3-d_6] (see Figure 4). The spectrum of the adsorbed iBA[3-d_6] represents a superposition of the solidlike and liquidlike line shapes at 115 K. The solidlike line with the quadrupole splitting of $(^3/_4)2\pi Q_1 = 38$ kHz and $\tau_R \gg [(^3/_4)2\pi Q_1]^{-1}$, i.e., $\tau_R \gg 4.2 \times 10^{-6}$ s, prevails at this temperature. This line belongs to the CD_3 group rapidly rotating about the C−C bond in the −CH−CD_3 fragment of the alcohol molecule. At 293 K, the liquidlike line with the width of 9.6 kHz and $\tau_R < [(^3/_4)2\pi Q_1]^{-1}$ provides the main contribution to the total spectrum.

For the CD_3 group rapidly rotating about the C−C bond, $\tau_{||}$ is usually about $10^{-10}-10^{-11}$ s (see, e.g., ref 41), whereas for the adsorbed alcohol, τ_R was estimated above to be $\sim 10^{-6}$ s. Hence, the conditions $\omega_I^2\tau_R^2 \gg 1$ and $\omega_I^2\tau_{||}^2 \ll 1$ ($\omega_I^2 = 1.49 \times 10^{17}$ rad^2/s^2) are valid for adsorbed iBA[3-d_6]. According to Boddenberg et al.,[6,39] the line width for a rapidly rotating methyl group $\Delta\nu_{1/2}(CD_3)$ is $^1/_9$ of the line width for a CD_2 (or CD) group, $\Delta\nu_{1/2}(CD_2)$, provided that $\tau_{||} \ll \tau_R < [(3/4)2\pi Q_1]^{-1}$. If τ_R decreases and approaches $\tau_{||}$, then $\Delta\nu_{1/2}(CD_2)$ will approach $\Delta\nu_{1/2}(CD_3)$, so that the condition $\Delta\nu_{1/2}(CD_2) \geq \Delta\nu_{1/2}(CD_3)$ is always valid.[6,38−40] Therefore, we also can expect that $\Delta\nu_{1/2}(CD_3)$ should be about $^1/_9\Delta\nu_{1/2}(CD_2)$ in Figures 3 and 4.

However, the observed $\Delta\nu_{1/2}(CD_3)$ is 9.6 kHz for iBA[3-d_6] at 293 K, i.e., the ratio $\Delta\nu_{1/2}(CD_3)/\Delta\nu_{1/2}(CD_2) = 9.6/45 \approx 0.21$. The deviation from the expected value of $1/9 \approx 0.11$ can be attributed to the additional mode of the C−CD_3 group motion, for example, to random changes (with respect tothe external magnetic field $\mathbf{B_0}$) in the orientation of the direction of the C−C bond between the CD_3 and CH groups of adsorbed iBA[3-d_6] (this mode of motion will be referred to as the librations of the CD_3 group). Moreover, one cannot exclude, a priori, that the observed liquidlike line shape with $\tau_R < [(^3/_4)2\pi Q_1]^{-1}$ ($\tau_R \sim 10^{-6}$ s) represents a superposition of several lines with different widths.

To substantiate the last suggestion, we have performed inversion−recovery experiments for CD_3 groups in the adsorbed iBA[3-d_6] at 133−293 K (these experiments are usually used for the determination of T_1 values in pulsed NMR spectroscopy[28]) (Figures 5 and 6). As seen from the spectral deconvolution presented in Figures 7 and 8, the observed ^{2}H NMR line shapes in Figures 4−6 can be considered as a superposition of three lines. Taking into account this deconvolution, we conclude that the liquidlike signal in Figures 4−6 represents a superposition of two lines, different in their line widths (T_2) and spin−lattice relaxation times (T_1).

At 153 K (Figures 5 and 8), in addition to the solidlike line (line III) with $\tau_R \gg [(^3/_4)2\pi Q]^{-1}$, there exist two more liquidlike lines: the line with $\Delta\nu_{1/2}(CD_3) = 10$ kHz and $\tau_0 \approx 14$ ms (line I) and the line with $\Delta\nu_{1/2}(CD_3) = 18$ kHz and $\tau_0 \approx 3.5$ ms (line II). Recall that τ_0 is the time at which the intensity of the observed signal in the inversion−recovery experiment is equal to zero (pulse sequence *ii*).

At 293 K, the two liquidlike lines in Figure 6 exhibit the following line widths and τ_0 values: $\Delta\nu_{1/2}(CD_3) = 6$ kHz and $\tau_0 \approx 95$ ms (line I) and $\Delta\nu_{1/2}(CD_3) = 15$ kHz and $\tau_0 \approx 40$ ms (line II). At 293 K, the $\Delta\nu_{1/2}(CD_3)/\Delta\nu_{1/2}(CD_2)$ ratios are about 0.13 and 0.33 for lines I and II, respectively, i.e., at least one of the ratios differs from the $^1/_9$ value. Recall that, in the absence of contributions from additional motions to the line width of the methyl group, this ratio should be equal to $^1/_9$. Thus, we can conclude that the line width of line II, and to a lesser extent of line I, may be affected by the libration of the C−CD_3 bond.

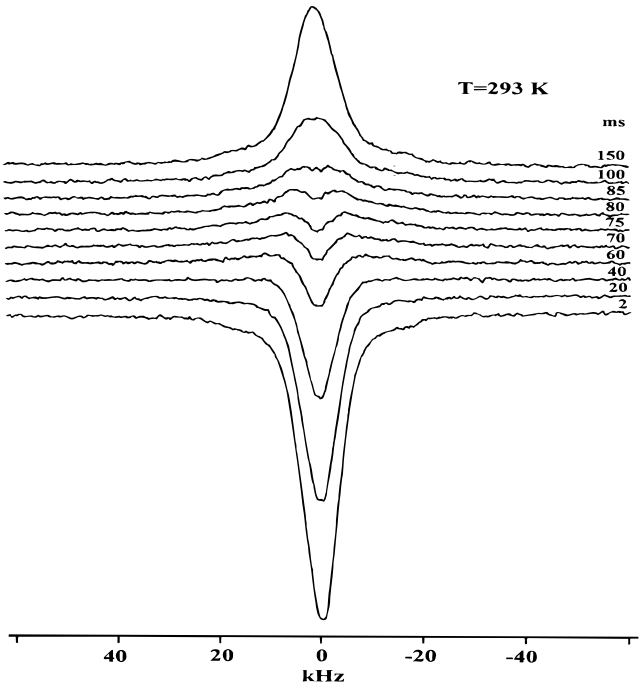

Figure 6. ^{2}H NMR inversion−recovery spectra recorded at 293 K for the CD_3 group of iBA[3-d_6] adsorbed on H-ZSM-5 (Si/Al = 24). The amount of adsorbed alcohol is 287 μmol/g. The delay time t_V (ms) is given above each spectrum.

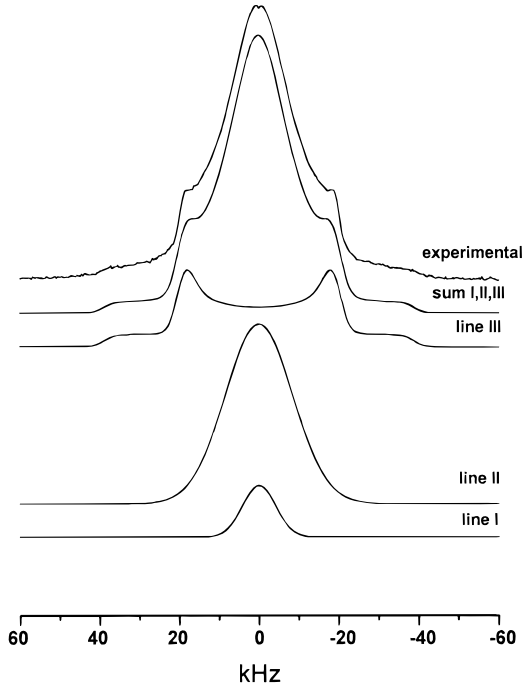

Figure 7. Simulation of the ^{2}H NMR line shape for iBA[3-d_6] on H-ZSM-5 at 133 K as a superposition of two liquidlike and one solidlike lines I−III.

A solidlike line III, from the CD_3 group rapidly rotating about C−C bond, exhibits the quadrupole splitting ($^3/_4$)Q_1 of 38 kHz (Figures 7 and 8), which corresponds to the quadrupole constant Q_0 = 152 kHz. This quadrupole constant is slightly less than typical values of Q_0 in CD_3 (CD_2) groups (165 kHz[31,32]). This diminishing of Q_0 may arise from the *fast* libration of the C−CD_3 bond. According to eq 2, the order parameter S is equal 0.921 for line III in a free diffusion in a cone model. Thus, the C−CD_3 bond in this fragment deviates by the angle $\gamma_0 \sim 19°$ from its mean position while librating in a cone.

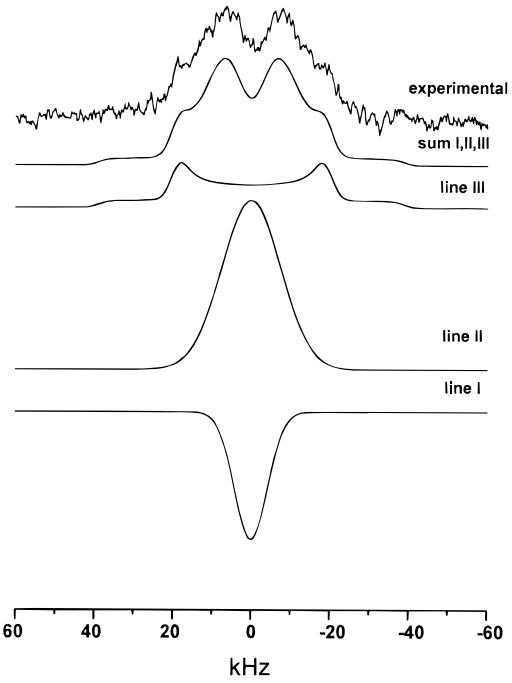

Figure 8. Simulation of ^{2}H NMR inversion−recovery spectrum of iBA[3-d_6] on H-ZSM-5 at 153 K with t_V = 6 as a superposition of two liquidlike and one solidlike lines I−III.

As for iBA[1-d_2], the three different lines for the CD_3 groups should be assigned to the three adsorption states of the alcohol in the zeolite. We assign lines I−III to the adsorption states I−III of the alcohol, correspondingly. It should be noted that we were able to identify only two adsorption states from the ^{2}H NMR spectra of iBA[1-d_2], whereas three adsorption states were reliably identified in the case of iBA[3-d_6]. We believe that our inability to identify three signals for iBA[1-d_2] may be related to the difficulties of unambiguous deconvolution of the spectrum of iBA[1-d_2] in Figure 3 into the three components, as well as to the difficulty in providing good spectra for the inversion−recovery experiment, in which two liquidlike signals could be distinguished.

Additional information on the dynamic behavior of the methyl groups in the three different adsorption states of the alcohol can be derived from an analysis of the temperature dependence of the spin−lattice relaxation times T_1 for lines I−III. T_1 for lines I and II is defined by the eq 9, whereas for line III, it is defined by eq 7 or 8. For each of the lines I−III, T_1 times were calculated from the τ_0 values obtained in the inversion−recovery experiments using on the equation $T_1 = \tau_0/\ln 2$.

Figures 9−11 show the temperature dependencies of T_1 for lines I−III, corresponding to the three different dynamic states of the methyl groups of the adsorbed iBA[3-d_6] alcohol. These dependencies were fit theoretically using correlation times τ_R, estimated earlier from the ^{2}H NMR line shape analysis for the adsorbed iBA[1-d_2] and assuming that parameters $D_{||}$, τ_P, τ_S, and τ_j (see eqs 7−9) have Arrhenius-type temperature behavior, i.e., $D_{||} = D_{||0} \exp(-E_{||}/RT)$, $\tau_j = \tau_{j0} \exp(E_j/RT)$, $\tau_P = \tau_{P0} \exp(E_P/RT)$, and $\tau_S = \tau_{S0} \exp(E_S/RT)$. The calculated order parameters, activation energies, and preexponential factors for methyl group rotation and libration in the three different dynamic states of the adsorbed alcohol are given in Table 1.

The temperature dependence of T_1 for line I is best fit with eq 9 provided that $\tau_S \ll \tau_P$ (Figure 9). The inequality $\tau_S \ll \tau_P$ reflects the fact that, in this case, the contribution from the fast libration of the methyl group to T_1 is negligible (the libration affects only the line shape), and the temperature dependence of

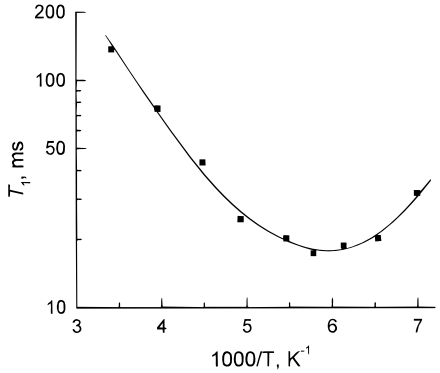

Figure 9. Temperature dependence of ^{2}H NMR spin−lattice relaxation time T_1 for the liquidlike line I of iBA[3-d_6] on H-ZSM-5. The solid line represents the theoretical fit to T_1 on the basis of eq 9 with the dynamic characteristics given in the Table 1.

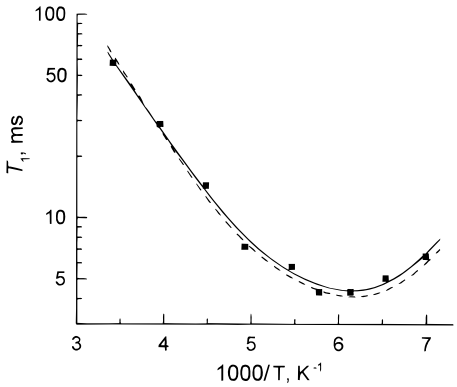

Figure 10. Temperature dependence of ^{2}H NMR spin−lattice relaxation time T_1 for the liquidlike line II of iBA[3-d_6] on H-ZSM-5. The dashed and solid lines represent theoretical fits (fit 1 and fit 2, respectively) to T_1 on the basis of eq 9 with the dynamic characteristics given in the Table 1.

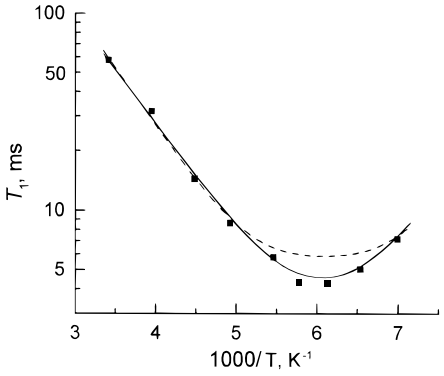

Figure 11. Temperature dependence of ^{2}H NMR spin−lattice relaxation time T_1 for the solidlike line III of iBA[3-d_6] on H-ZSM-5. The solid line represents a theoretical fit to T_1 on the basis of the three-site jump model (eq 8), whereas the dashed line is a theoretical fit to T_1 on the basis of one-axis rotational diffusion model (eq 7) with the dynamic characteristics given in the Table 1.

T_1 is defined predominantly by the temperature dependence of the correlation time τ_P for one-axis rotational diffusion of the methyl group about the C−CD_3 bond with the activation energy $E_P = 11.1$ kJ/mol. The rather small magnitude of the order parameter ($S = 0.497$, see Table 1) indicates large-amplitude librations of the methyl groups of the alcohol in adsorption state I. This value of the order parameter corresponds to diffusion in a cone with semiangle $\gamma_0 \approx 52°$ for the free diffusion in a cone model for C−CD_3 bond motion. The motion of the C−CD_3 bond vector is definitely much more complex then expected from the simplest free diffusion in a cone model. Considerable efforts, probably the use of molecular dynamics simulations, are necessary to reveal the detailed picture of such motion. By suggesting that, inside the zeolite, the *iso*-butyl alcohol molecule is bound to the zeolite hydroxyl group Si−OH−Al between rare jumps, it is possible to explain significant deviations of the C−CD_3 bond from its mean direction only by assuming some hindered rotations about the CH−CH_2 and/or CH_2−OH bonds, which effectively provide large-amplitude librations of the CD_3 group.

The interpretation of the spin−lattice relaxation data for line II is more ambiguous. The temperature dependence of T_1 may be well-fit in at least two different ways (see fits 1 and 2 in Table 1 and Figure 10). Fit 1 corresponds to fast one-axis uniform rotation of the methyl group without any librations ($S = 1$) and with $\tau_P \ll \tau_R < [(^3/_4)2\pi Q_1]^{-1}$, provided that the alcohol molecule slowly reorients isotropically with $\tau_R \sim 1 \times 10^{-6}$ s. In contrast, fit 2 contains a contribution to T_1 from the methyl group librations and is characterized by the significantly smaller order parameter $S = 0.2$ (all other parameters are given in Table 1). The ratio $\Delta\nu_{1/2}(CD_3)/\Delta\nu_{1/2}(CD_2)$ is equal to 0.133 for line II and is close to the expected $^1/_9$ value in the case of $S = 1$ and $\tau_{||} \ll \tau_R < [(^3/_4)2\pi Q_1]^{-1}$ (vide supra). Nevertheless, the complete absence of librations of the CD_3 group in a molecule undergoing isotropic reorientation and possessing a liquidlike ^{2}H NMR spectrum is unlikely. In this respect, fit 2 with $S = 0.2$ is preferable. The small value of the order parameter corresponds to the large amplitude of the alcohol methyl groups librations ($\gamma_0 \sim 72°$), as in the previous case for line I.

For the solidlike line III with $\tau_R \gg [(^3/_4)2\pi Q_1]^{-1}$, the temperature dependence of T_1 for the perpendicular component of the spectrum ($\chi = \pi/2$) was fit by two different models of CD_3 group motion, rotational diffusion and three-site jumps about the C−CD_3 axis on the basis of eqs 7 and 8, respectively. As seen from Figure 11, the three-site jump model of the methyl group motion with $E_j = 10.5$ kJ/mol and $\tau_{j0} = 2.7 \times 10^{-12}$ s (Table 1) fits the experimental points more accurately than the one-axis rotational diffusion model. As shown above, the order parameter S estimated from a comparison of the observed quadrupole splitting with the value of 41.25 kHz expected for the deuterium nucleus in a rapidly rotating CD_3 group with a typical quadrupole coupling constant $Q_0 = 165$ kHz,[31,32] is $S = 0.921$ (this value of S corresponds to $\gamma_0 = 19°$ for free diffusion in a cone). Thus, *iso*-butyl alcohol molecule in adsorption state III can be considered as rigid (or slowly reorienting with $\tau_R \gg 4.2 \times 10^{-6}$ s) on the ^{2}H NMR time scale. The methyl groups of this molecule undergo fast rotation about the C−CD_3 bond, most likely by means of three-site jumps, and simultaneously, the C−CD_3 bond undergoes fast libration with the small angle $\gamma_0 \sim 19°$.

Discussion

It follows from the experiments with iBA[3-d_6] that *iso*-butyl alcohol adsorbed on zeolite H-ZSM-5 exhibits an ^{2}H NMR spectrum that represents a superposition of three signals. Three signals correspond to alcohol molecules that differ in their dynamic behavior inside the H-ZSM-5 zeolite framework. On one hand, adsorbed *iso*-butyl alcohol molecules differ by the estimated correlation time τ_R of isotropic reorientation of the molecule as a whole (Table 1), which is more than 10^{-6} s for all three adsorption states. This time can be related to the translational motion of the alcohol molecules along the zeolite channels. On the other hand, the alcohol molecules differ by the mode of methyl group mobility, which represents a

TABLE 1: Dynamic Characteristics for Three Adsorption States of *Iso*-butyl Alcohol in Zeolite H-ZSM-5[a]

	adsorption state I line I	adsorption state II line II		adsorption state III line III	
		fit 1	fit 2	diffusion model	3-site jump model
S	0.497	1	0.200	0.921	0.921
γ_0	52°	0	~72°	~19°	~19°
τ_R, s (293 K)	$\sim 1 \times 10^{-6}$	$\sim 1 \times 10^{-6}$	$\sim 1 \times 10^{-6}$	$\gg 4.2 \times 10^{-6}$	$\gg 4.2 \times 10^{-6}$
D_{ll0}, s^{-1}				1.12×10^{12}	
τ_{j0}, s					2.7×10^{-12}
τ_{P0}, s	2.7×10^{-13}	1.2×10^{-13}	1.17×10^{-13}		
τ_{S0}, s	$\tau_S \ll \tau_P$	$\tau_S \ll \tau_P$	2.8×10^{-13}		
E_{ll}, kJ/mol				11.4	
E_j, kJ/mol					10.5
E_P, kJ/mol	11.1	11.9	11.9		
E_S, kJ/mol			14.5		

[a] Each of the lines I−III in Figures 7 and 8 corresponds to the adsorption states I−III inside the zeolite channels.

combination of two modes of the motion: one-axis rotation of the methyl group about the C−CD_3 bond and, at least for adsorption states I and II, large deviations (librations) of this axis from its mean direction. Some combined hindered rotations about the CH−CH_2 and CH_2−OH bonds are most likely responsible for the C−CD_3 bond librations.

The main adsorption sites for *iso*-butyl alcohol inside zeolite H-ZSM-5 represent bridged OH groups (Al−OH−Si groups), which can be located both inside the channels and at the channel intersections.[42] Therefore, it is reasonable to assume that peculiarities of the adsorbed alcohol dynamics may be connected with the location of the acidic Al−OH−Si groups inside the zeolite channel system. Close-to-isotropic *effective* reorientation may occur by random jumps of the molecule among Al−OH−Si groups. As long as there is an average of no more than one acidic site per channel intersection for the zeolite samples under study and some of the acidic OH groups are located inside the channels, we suppose that Al−OH−Si groups located both inside the channels and at channel intersections may participate in the isotropic reorientation of the alcohol molecule. Taking into account that the *iso*-butyl alcohol molecule dimensions and the diameter of ZSM-5 zeolite channels are comparable (ca. 5.5 Å[19]), it is possible to make additional assumptions and to assign the three observed ^{2}H NMR signals to some certain adsorption sites. Lines I and II most likely belong to the molecules adsorbed on Al−OH−Si groups located at channel intersections. Sufficient space exists at the channel intersection void (diameter of the channel intersection is about 9 Å[19]) for the adsorbed alcohol molecule to fulfill the large amplitude librations. Different locations of the acidic OH groups near channel intersections may result in a slightly different spatial surroundings for the adsorbed alcohol molecule. This may be sufficient to produce a difference in the amplitude of the methyl group librations, which manifests itself as lines I and II in the ^{2}H NMR spectrum. Line III may be assigned to the alcohol molecules more strongly adsorbed on the OH groups located inside the zeolite channels and/or possessing additional van der Waals interactions between the alcohol hydrogen atoms and the zeolite lattice oxygens. This prevents the methyl groups of bulky *iso*-butyl alcohol from involvement in librations of large amplitude.

Theoretical studies of the energetics of butyl alcohol adsorption on Si−OH−Al groups of H-ZSM-5[18] have shown only small variations in adsorption energies with respect to different crystallographic positions of the zeolite for all isomeric butyl alcohols. This is in a good agreement with our ^{2}H NMR observations of three different adsorption states for *iso*-butyl alcohol.

It is evident from Table 1 that the activation energies for CD_3 group rotation are also similar and differ by no more than 1.5 kJ/mol in all cases. Note also that the ratio between the intensities of the solidlike and liquidlike signals changes with an increase in temperature in favor of the latter (Figures 3 and 4). This can be reasonably explained by the temperature redistribution of alcohol molecules inside the zeolite structure, corresponding to their preferable migration from channels to channel intersections, where they have sufficient space to be involved in large-amplitude local motion.

Thus, by using ^{2}H NMR spectroscopy, it is possible to discriminate distinctly between different adsorption states of *iso*-butyl alcohol in zeolite H-ZSM-5 that are, in fact, very similar in the adsorption energy.[18] The alcohol molecules adsorbed on these adsorption sites are different in their motional behavior. The ^{2}H NMR line shape and T_1 relaxation data analysis of the three observed different signals of adsorbed alcohol allows us to assign these signals to some certain alcohol positions inside the channels or at channel intersections in the framework of H-ZSM-5. Moreover, ^{2}H NMR spectroscopy allowed us to obtain additional information on the peculiarities of the motional behavior (especially intramolecular) of the *iso*-butyl alcohol molecules adsorbed on bridged OH groups.

Conclusions

The following conclusions can be drawn from ^{2}H NMR studies of the mobility of *iso*-butyl alcohol inside the channels of H-ZSM-5 zeolite. Adsorbed deuterated the alcohol exhibits ^{2}H NMR line shape that represents a superposition of the three signals: two liquidlike lines and one solidlike line. The liquidlike signals probably belong to the alcohol molecules adsorbed on differently located Al−OH−Si groups at channel intersections. Both of these types of alcohol molecules reorient isotropically with the correlation time $\tau_R \sim 1 \times 10^{-6}$ s. They differ in the amplitude of the methyl groups librations, which is large for both adsorption states: $\gamma_0 \sim 52°$ for one of them and $\gamma_0 \sim 72°$ for another one. The solidlike signal is assigned to the alcohol molecules adsorbed on acidic Al−OH−Si groups located inside the zeolite channels. These alcohol molecules reorient isotropically with $\tau_R > 4.2 \times 10^{-6}$ s and exhibit small amplitude, fast librations of methyl group with $\gamma_0 \sim 19°$. All three observed physisorption states of *iso*-butyl alcohol have similar adsorption energies, for which adsorbed molecules are also characterized

by similar activation energies and rates of methyl group rotational diffusion or jumps about $C-CD_3$ bond.

Acknowledgment. The authors are grateful to Dr. V. N. Romannikov for synthesis of the samples of zeolite H-ZSM-5. Synthesis of ^2H selectively labeled *iso*-butyl alcohols by V. N. Zudin is gratefully acknowledged. This research was made possible with financial support from INTAS (Grant 96-1177).

References and Notes

(1) Hasha, D. L.; Miner, V. W.; Garces, J. M.; Rocke, S. C. In *Catalysts Characterization Science*; Deviney, M. L., Gland, J. L., Eds.; ACS Symposium Series 288, American Chemical Society: Washington, DC, 1985; p 485.

(2) Eckman, R. R.; Vega, A. J. *J. Phys. Chem*. **1986**, *90*, 4679.

(3) Luz, Z.; Vega, A. J. *J. Phys. Chem*. **1987**, *91*, 374.

(4) (a) Newsam, J. M.; Silbernagel, B. G.; Garcia, A. R.; Hulme, R. *J. Chem. Soc., Chem. Commun.* **1987**, 664. (b) Alexander, P.; Gladden, L. F. *Zeolites* **1997**, *18*, 38.

(5) Boddenberg, B.; Burmeister, R. *Zeolites*, **1988**, *8*, 480.

(6) Boddenberg, B.; Burmeister, R. *Zeolites*, **1988**, *8*, 488.

(7) Kustanovich, I.; Fraenkel, D.; Luz, Z.; Vega, S.; Zimmermann, H. *J. Phys. Chem*. **1988**, *92*, 4134.

(8) Kustanovich, I.; Vieth, H. M.; Luz, Z.; Vega, S. *J. Phys. Chem*. **1989**, *93*, 7427.

(9) Silbernagel, B. G.; Garcia, A. R.; Newsam, J. M.; Hulme, R. *J. Phys. Chem*. **1989**, *93*, 6506.

(10) Burmeister, R.; Boddenberg, B.; Verfürden, M. *Zeolites* **1989**, *9*, 318.

(11) Stepanov, A. G.; Maryasov, A. G.; Romannikov, V. N.; Zamaraev, K. I. *Magn. Reson. Chem*. **1994**, *32*, 16.

(12) Stepanov, A. G.; Shubin, A. A.; Luzgin, M. V.; Jobic, H.; Tuel, A. *J. Phys. Chem. B* **1998**, *102*, 10860.

(13) Sato, T.; Kunimori, K.; Hayashi, S. *Phys. Chem. Chem. Phys*. **1999**, *1*, 3839.

(14) Dwyer, J. *Nature (London)* **1989**, *339*, 174.

(15) (a) Aronson, M. T.; Gorte, R. J.; Farneth, W. E. *J. Catal*. **1987**, *105*, 455. (b) Aronson, M. T.; Gorte, R. J.; Farneth, W. E.; White, D. *J. Am. Chem. Soc*. **1989**, *111*, 840. (c) Lazo, N. D.; Richardson, B. R.; Schettler, P. D.; White, J. L.; Munson, E. J.; Haw, J. F. *J. Phys. Chem*. **1991**, *95*, 9420.

(16) (a) Williams, C.; Makarova, M. A.; Malysheva, L. V.; Paukshtis, E. A.; Zamaraev, K. I.; Thomas, J. M. *J. Chem. Soc., Faraday Trans*. **1990**, *86*, 3473. (b) Makarova, M. A.; Williams, C.; Romannikov, V. N.; Thomas, J. M.; Zamaraev, K. I. *J. Chem. Soc., Faraday Trans.* **1990**, *86*, 581. (c) Makarova, M. A.; Williams, C.; Thomas, J. M.; Zamaraev, K. I. *Catal. Lett*. **1990**, *4*, 261. (d) Williams, C.; Makarova, M. A.; Malysheva, L. V.; Paukshtis, E. A.; Talsi, E. P.; Thomas, J. M.; Zamaraev, K. I. *J. Catal*. **1991**, *127*, 377.

(17) (a) Stepanov, A. G.; Romannikov, V. N.; Zamaraev, K. I. *Catal. Lett*. **1992**, *13*, 395. (b) Stepanov, A. G.; Zamaraev, K. I.; Thomas, J. M. *Catal. Lett*. **1992**, *13*, 407. (c) Stepanov, A. G.; Zamaraev, K. I. *Catal. Lett*. **1993**, *19*, 153.

(18) Shubin, A. A.; Catlow, C. R. A.; Thomas, J. M.; Zamaraev, K. I. *Proc. R. Soc. London A* **1994**, *446*, 411.

(19) (a) Olson, D. H.; Kokotailo, G. T.; Lawton, S. L.; Meier, W. M. *J. Phys. Chem*. **1981**, *85*, 2238. (b) Kokotailo, G. T.; Lawton, S. L.; Olson, D. H.; Meier, W. M. *Nature (London)* **1978**, *272*, 437. (c) Flanigen, E. M.; Bennett, J. M.; Grose, R. W.; Cohen, J. P.; Patton, R. L.; Kirchner, R. M.; Smith, J. V. *Nature (London)* **1978**, *271*, 512.

(20) Speiss, H. W. Rotation of Molecules and Nuclear Spin Relaxation. In *NMR Basic Principles and Progress*; Diehl, P., Fluck, E., Kosfeld, R., Eds.; Springer-Verlag: New York, 1978; Vol. 15, p 55.

(21) Mehring, M. Principles of High-Resolution NMR in Solids. In *NMR Basic Principles and Progress*; Diehl, P., Fluck, E., Kosfeld, R., Eds.; Springer-Verlag: New York, 1976; Vol. 11.

(22) Abragam, A. *The Principles of Nuclear Magnetism*; Oxford University Press: Oxford, U.K., 1961.

(23) Romannikov, V. N.; Mastikhin, V. M.; Hočevar, S.; Držaj, B. *Zeolites* **1983**, *3*, 313.

(24) Fyfe, C. A.; Gobbl, G. C.; Hartman, J. S.; Klinowski, J.; Thomas, J. M. *J. Phys. Chem*. **1982**, *86*, 1247.

(25) (a) Powles, J. G.; Strange, J. H. *Proc. Phys. Soc*. **1963,** *82*, 6. (b) Davis, J. H.; Jeffery, K. R.; Bloom, M.; Valic, M. I.; Higgs, T. P. *Chem. Phys. Lett*. **1976**, *42*, 390.

(26) Bloom, M.; Davis, J. H.; Valic, M. I. *Can. J. Phys*. **1980**, *58*, 1510.

(27) Lin, T.-H.; Vold, R. R.; Vold, R. L. *J. Magn. Reson*. **1991**, *95*, 71.

(28) Farrar, T. C.; Becker, E. D. *Pulse and Fourier Transform NMR. Introduction to Theory and Methods*; Academic Press: New York, 1971.

(29) Smith, I. C. P. Deuterium NMR. In *NMR of Newly Accessible Nuclei*; Laszlo, P., Ed.; Academic Press: London, 1983; Vol. 2, p 1.

(30) Jelinski, L. W. Deuterium NMR of Solid Polymers. In *High-Resolution NMR Spectroscopy of Synthetic Polymers in Bulk (Methods and Stereochemical Analysis)*; Komoroski, R. A., Ed.; VCH Publishers: New York, 1986; Vol. 7, p 335.

(31) Barnes, R. G. *Adv. Nucl. Quadrupole Reson*. **1974**, *1*, 335.

(32) Rinne, M.; Depireux, J. *Adv. Nucl. Quadrupole Reson*. **1974**, *1*, 357.

(33) Stocktone, G. W.; Polnaszek, C. F.; Tulloch, A. P.; Hasan, F.; Smith, I. C. P. *Biochemistry* **1976**, *15*, 954.

(34) Mantsch, H. H.; Saito, H.; Smith, I. C. P. *Prog. Nucl. Magn. Reson. Spectrosc.* **1977**, *11*, 211.

(35) Boddenberg, B.; Grosse, R. *Z. Naturforsch., A* **1986**, *41*, 1361.

(36) Petersen, N. O.; Chan, S. I. *Biochemistry* **1977**, *16*, 2657.

(37) Wittebort, R. J.; Szabo, A. *J. Chem. Phys*. **1978**, *69*, 1722.

(38) Torchia, D. A.; Szabo, A. *J. Magn. Reson*. **1982**, *49*, 107.

(39) Boddenberg, B.; Beerwerth, B. *J. Phys. Chem*. **1989**, *93*, 1440.

(40) Brainard, J. R.; Szabo, A. *Biochemistry* **1981**, *20*, 4618.

(41) (a) Keniry, M. A.; Kintanar, A.; Smith, R. L.; Gutowsky, H. S.; Oldfield, E. *Biochemistry* **1984**, *23*, 288. (b) Kintanar, A.; Alam, T. M.; Huang, W. Ch.; Schindele, D. C.; Wemmer, D. E.; Drobny, G. *J. Am. Chem. Soc.* **1988**, *110*, 6367.

(42) Schröder, K.-P.; Sauer, J.; Leslie, M.; Catlow, C. R. A. *Zeolites* **1992**, *12*, 20.